

JPMTR 112 | 1812
DOI 10.14622/JPMTR-1812
UDC 655.1+621.38(004.35)

Research paper
Received: 2018-06-20
Accepted: 2018-09-04

Effect of printing parameters on microwave performance of printed chipless RFID tags

Sika Shrestha and Nemai Chandra Karmakar

Department of Electrical and Computer System Engineering,
Monash University, Australia

sika.shrestha@monash.edu
nemai.karmakar@monash.edu

Abstract

The chipless Radio Frequency Identification system (RFID) will revolutionize the identification market due to its low-cost tagging methods. The printed version of the chipless tag is able to reduce the cost to few cents per tag. The microwave performance of the printed chipless tag is suffered due to the practical limitations of the overall fabrication procedure through printing. The bandwidth broadening is unavoidable for the printed tag, which directly hits on the data capacity. Similarly, the strength of the microwave signal is also degraded for printed RFID tag, which affects the reading distance of the tag. The fabrication of chipless RFID tag via printing involves several parameters such as the conductive ink processing condition, the substrate parameters and the geometrical dimension of the printed tag. We need to understand the relationship between these printing parameters with the microwave response of the printed tag, to analyze the key parameters affecting the response of the printed tag. A comprehensive experimental investigation is performed in this paper to evaluate the relationship between the printing parameters and microwave response of the printed tag. The printing parameters include conductive ink sintering type and sintering conditions and deposited ink thickness. A high-speed photonic sintering process is adopted for the first time to sinter chipless RFID tag so that chipless RFID tag can be manufactured using fast roll-to-roll printing process. Optimum conditions for the photon-sintering process are deduced through experimental analysis for conductive inks of various viscosity. The effect of the geometrical dimensions of the printed strip and the printing accuracy is also analyzed to understand the limitations of the printing technique in terms of tag size. The issues seen in the printed RFID tag, their reason and the solution is then deduced in the final section so that the printed chipless tag can accommodate the real world limitations to make viable commercial outcome.

Keywords: RFID communication, screen-printing technology, conductive ink, oven sintering, photon sintering

1. Introduction

Chipped Radio Frequency Identification (RFID) system is not able to compete with ubiquitous barcode system and make a remarkable position in the market for automatic identification and data capture technology owing to its higher cost and non-planar nature of RFID tag. A minimum cost of five cents is achievable for chipped RFID tag, only in the case of mass production. The high volume customers such as Walmart uses several hundreds of millions of tags per year. However, the tag price of 5 cents to 10 cents is still too expensive for low-cost applications. The low price items with low-profit margins can only be tagged using the tag costing a fraction of a cent. Also, the structure of chip makes the RFID tag non-planar, which does not allow it to be used on commercial substrates such as banknotes and other

paper documents. A new domain of RFID system which does not require the chip for data encoding in RFID tag is able to reduce the tag cost and make it planar. The removal of the chip in the chipless tag has made it planar and provided an opportunity for obtaining a fully functional printed RFID tag for many low-cost applications. This chipless RFID tag can act as RF barcodes if they are printed on flexible substrates and on commercial items like a barcode. The tag cost can be significantly lowered through manufacturing of chipless tag using an additive, high-throughput printing process, and low-cost conductive inks. It has been predicted by Das and Harrop (2010) that 624 billion chipless tags will be sold in 2019 if the targeted low cost is achieved.

The data encoding in a chipless RFID system is based on the electromagnetic signature since there is no chip

or memory to store the tag identification data (tag ID). The identification data generated by the chipless tag can be based on frequency signature (Preradovic and Karmakar, 2009; Khan, Tahir, and Cheema, 2016; Noor, et al., 2016; Sajitha, et al., 2016; Huang and Su, 2017), time domain reflectometry (Chamarti and Varahramyan, 2006; Forouzandeh and Karmakar, 2015; Mandel, et al., 2015), image domain (Zomorodi, 2015), and phase domain (Balbin and Karmakar, 2009; Genovesi, et al., 2014; 2016). The frequency signature based chipless RFID tags are multi-resonator tags, where each resonator encodes 1 bit. The presence of resonance in predetermined frequency is identified as a data bit. The resonator exhibits the frequency selective behaviour and abrupt spectral features in amplitude spectrum are used to encode digital data bits. The chipless RFID tags based on time domain reflectometry identify the tag ID in the form of the delay in the train of echoes to an interrogation signal sent by the reader. The presence and absence of resonator in the tag are identified using the unique electromagnetic (EM) image in image domain based chipless RFID tag. The abrupt spectral features in the phase spectrum exhibited by the resonator are considered as the tag ID for data encoding based on phase domain.

Various printed chipless RFID tags have been reported in the literature (Vena, et al., 2013; 2014; Borgese, et al., 2017; Jeon, et al., 2017; Herrojo, et al., 2018) but the issues seen in printed tag response during the fabrication of chipless RFID tag via printing are not explored in detail. To understand the issues with the response from the printed tag, the relationship between the various parameters involved in the printing process and the microwave response needs to be analyzed. In this paper, chipless RFID tag generating the tag ID in the frequency domain is printed using screen-printing technology. The microwave response of the printed tag is analyzed to investigate the effect of various printing parameters on the performance of chipless RFID tag.

The printing of chipless RFID tags involves two main steps: printing and sintering (annealing). The printing is performed using a commercial printing technique such as screen-printing and ink-jet printing using conductive ink. The metal paste or liquid metal which are mixed with binders that help the ink to remain attached to the substrate surface are used as conductive inks for printing of chipless tags. The solid content of silver in these inks is not 100 per cent so they have low conductivity compared to relatively pure metals like copper or aluminium.

The parameters involved in the fabrication of printed RFID tag are shown in Figure 1. The paper is organised as per this figure. The deposited ink thickness can get varied during different printing procedures and the

effect of varying deposited ink thickness and optimum required thickness is analyzed in Section 2. The sintering process removes the resistive elements, forming the conductive path. The sintering of the printed sample is performed using oven sintering in Section 3. A high-speed photonic sintering process is applied on the printed tags in Section 4 to make the manufacturing of tags through printing, adaptable to the industrial roll-to-toll printing process. The effect of the ink processing conditions for various inks is examined for oven-sintered and photon-sintered printed tags in these sections. The effect of tag dimension on electrical parameters of the printed strip is shown in Section 5. The inaccuracy seen in printed dimensions is depicted in Section 7 with a possible solution. Finally, a dependency chart between the printed tag response and the printing parameters is explained in Section 8, which will assist in figuring out the bottleneck in obtaining a high fidelity printed tag response and assess the alteration required in the tag and the manufacturing process to enhance the printed tag response.

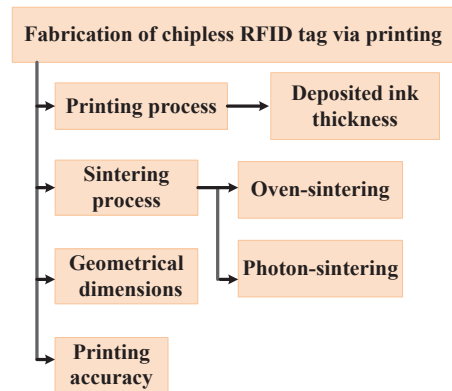


Figure 1: Various printing parameters affecting the microwave performance of printed chipless RFID tag

2. Effect of ink thickness on microwave performance of the printed tag

The conductor thickness of the printed tags is usually lower than the thickness of copper metallization in the Printed Circuit Board (PCB) fabricated tag. The thickness of ink deposited in printing process mainly depends on the printing technique and ink viscosity. The signal loss occurs when the deposited ink thickness is less than the skin depth at the operating frequency. This is because of the leakage of the microwave signal through the dielectric substrate layer for low conductive ink thickness which results in signal penetration loss as it propagates along the conducting guiding structure. The consequence is the spread of the quality factor of the resonator with strong negative impact on the data capacity of the resonator. In this section, the effect of ink thickness on the microwave performance

of printed tags has been analyzed and an approximate minimum thickness required to obtain acceptable microwave performance is evaluated. Initially, the rectangular bars of 2 mm width are printed using silver-based conductive ink named ‘SHR-2’. The details of ‘SHR-2’ ink are given in Table 1 (note: 1 mil = 25.4 μm). The sample is printed on polyethylene terephthalate (PET) substrate which can withstand up to 250 °C. The sheet resistance of the printed strip is measured using a four-point probe SRM-232. The sheet resistance of rectangular printed strips obtained for varying ink thickness is plotted in Figure 2. Five sheet resistance and five thickness values are averaged for sheet resistance and thickness values respectively in this section and all other following sections. The sheet resistance is inversely proportional to the deposited ink thickness. The resistance is low for higher thickness as the amount of conductive material is less for low thickness.

Table 1: Details of experimented conductive inks

Ink name	Metal content	Sintering conditions	Sheet resistance (Ω/sq/mil)
SHR-2	68.5 %	120 °C for 15 min	<0.010
SHR-1	84.0 %	110 °C for 5 min	<0.010
SHR-5	76.0 %	150 °C for 5 min	<0.005

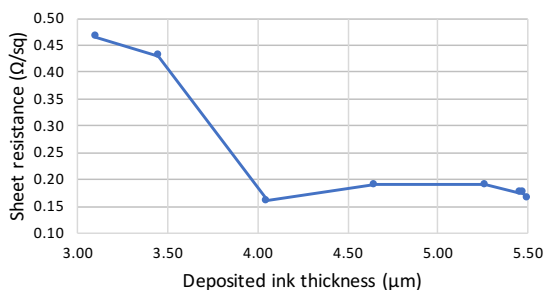


Figure 2: Sheet resistance for different deposited ink thicknesses (for a rectangular bar of width 2 mm, printed using ‘SHR-2’ ink on PET substrate, sintered at 120 °C for 15 min)

The modified version of Electric-LC (ELC) resonator (Naqui, et al., 2014) is considered as chipless RFID tag in this paper. The RFID tags printed using ‘SHR-2’ screen-printing ink on PET substrate tend to have different thickness because of manual screen printing. The thickness varied from 1 μm to 8 μm. The tag with at least 3 μm thickness gave detectable microwave response. The microwave performance of the chipless RFID printed tag can be evaluated in terms of 3 dB bandwidth and Radar Cross Section (RCS) amplitude as shown in Figure 3. The bandwidth is obtained as the frequency range that lies within 3 dB of the response at its peak. The electromagnetic response reflected from the tag is considered as the identification data in

the chipless RFID system and the reflected response is obtained in terms of RCS. The RCS amplitude is the strength of the received signal, which is the difference between the peak and null of the signal as shown in Figure 3.

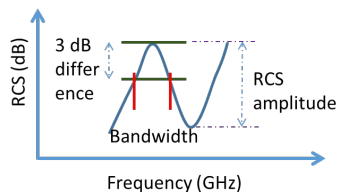


Figure 3: Illustration of bandwidth and radar cross section amplitude difference

The RCS amplitude and 3 dB bandwidth are obtained for the first resonant frequency (3.9 GHz) of the printed tags in this section and all following sections. In frequency coded chipless RFID tags, the bandwidth of the electromagnetic response needs to be low so that higher amount of data bits can get fitted within the given frequency range.

The higher value of RCS amplitude, which is the strength of the signal, increases the reading distance of the tag. The measured 3 dB bandwidth and RCS amplitude for varying ink thicknesses are depicted in Figure 4. The bandwidth is broadened for the chipless RFID tags compared to fabricated tag because of low conductivity of the ink. The bandwidth broadening is reduced for higher resonator thickness. The strength of the signal or the RCS amplitude has also risen for higher deposition of conductive ink. If we considered 250 MHz as the acceptable bandwidth for experimented tags in this section, then, the thickness of the resonator needs to be at least 6 μm.

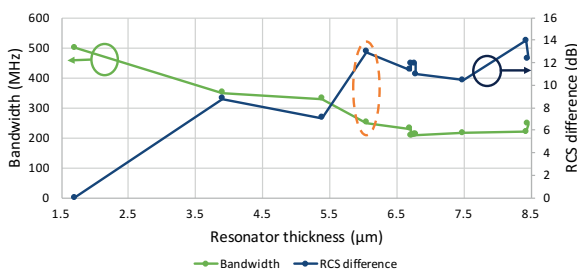


Figure 4: Microwave performance of RFID tags printed using ‘SHR-2’ ink for different deposited ink thicknesses

To understand the relation of the skin effect with the thickness of deposited ink, the skin depth is calculated for the frequency range from 4 GHz to 8 GHz for three different conductivity values and is shown in Figure 5. The conductivity obtained for this print is $1.8 \cdot 10^6$ S/m. The previous analysis shows that 6 μm are the minimum thickness required at 3.9 GHz. Figure 5 shows that at 3.9 GHz, the skin depth is around 6 μm. Hence,

the thickness of the deposited ink should be at least around the skin depth at the given frequency.

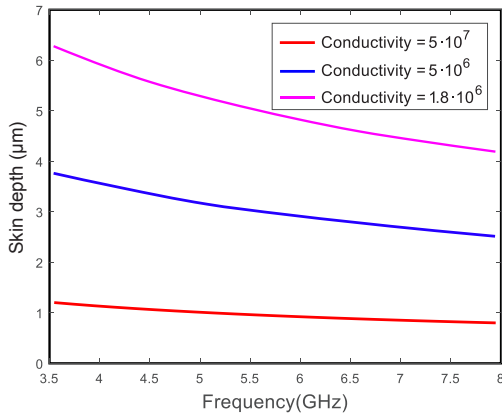


Figure 5: Skin depth versus frequency (3.5–8.0 GHz)

Therefore, the higher thickness of deposited conductive ink is desirable to obtain a response with low resistance, less bandwidth broadening, and higher RCS amplitude. The screen-printing technique is able to provide higher ink thickness compared to other printing techniques. A multiple passes of printing can be employed in other printing techniques such as ink-jet printing and gravure printing to increase the ink thickness.

3. Oven sintering of printed RFID tag

The microwave response of the chipless RFID tag, when printed using conductive ink, is highly dependent on the processing conditions of the ink. The conductive ink contains a resistive element such as dispersant material along with conductive metal pigment. The metal particles in the ink are surrounded by the dispersant material which keep the particles apart from each other and electrical conductivity does not form (Halonen, et al., 2013). These ink dispersants need to be removed in order to connect the conductive particles to form functional ink strips. The ink is passed through a heating process known as sintering to disorder/melt/evaporate the dispersant and other resistive solvents to form the conductive paths. The sintering process also promotes the formation and coalescence of printed conductive features, which improves the electrical conductivity and the mechanical adhesion (Lukacs, Pietriková, and Cabuk, 2017). This section investigates the relationship between the ink processing parameters and the microwave performance of the printed tags for oven-sintered samples.

The oven sintering process is strongly connected with the conditions of technological process temperature and time (Lukacs, Pietriková and Cabuk, 2017).

The screen-printed rectangular bar using ‘SHR-2’ ink and having 2 mm width was sintered at four different conditions. The sheet resistance and thickness were measured using the four-point probe (SRM-232) and optical profiler (Bruker contour GT-K), respectively, and the conductivity is calculated using Equation [1]

$$\sigma = \frac{1}{R_s \cdot t} \tag{1}$$

where σ is the conductivity, R_s is the sheet resistance and t is the thickness of deposited ink. Figure 6 shows the sheet resistance and conductivity of the printed bars.

The sheet resistance was significantly reduced from 0.4 Ω/sq to 0.1 Ω/sq when the sintering temperature increased from 80 °C to 120 °C and hence the conductivity increment is also noteworthy. The higher sintering temperature removes the higher amount of resistive component allowing more metal component to form a conductive path which thus increases the conductivity. The longer sintering time only brought a slight increment in the conductivity as seen for samples sintered at 80 °C/10 min and 80 °C/30 min. Hence, the sintering temperature plays a contributing role rather than sintering time to increase the conductivity of printed strips.

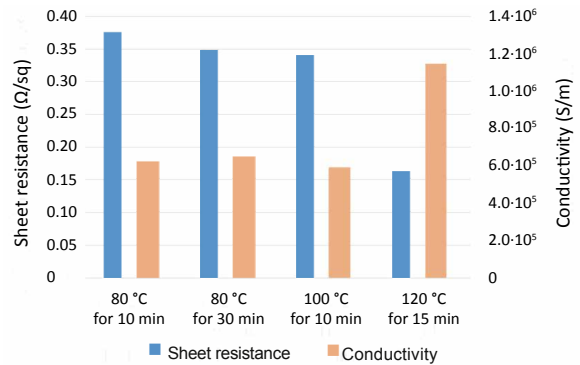


Figure 6: Conductivity obtained for printed strips sintered at different temperature of samples printed using ‘SHR-2’

The microwave performance of the printed chipless RFID tags was investigated in terms of RCS amplitude and 3 dB bandwidth (Figure 3) for varying ink processing conditions. The RCS amplitude and bandwidth of samples printed using ‘SHR-2’ ink and sintered at different temperatures is depicted in Figure 7. Since the conductivity of the ink is increased for higher sintering temperature, the bandwidth of the first peak is also decreased up to 212 MHz. The bandwidth broadening is unavoidable because of low conductivity of the ink. However, we can minimize the bandwidth broadening through the sintering of ink at a higher temperature. The strength of resonance is also improved for higher sintering temperature.

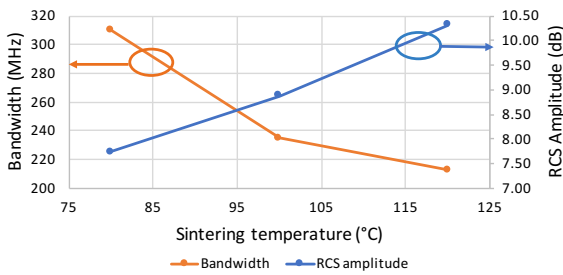


Figure 7: Microwave performance of RFID tags printed using 'SHR-2' ink for different sintering temperatures

The effect of sintering temperature on microwave performance of RFID tags printed using different inks is also investigated in Figure 8.

The higher sintering temperature of the conductive ink does not guarantee the enhanced microwave performance of the printed RFID tag. It also depends on the ink composition and formulation of the conductive ink procured from the ink supplier. Another ink supplier whose ink is named 'SHR-1' has stated its metal content as 84 % and recommended sintering temperature as 110 °C/5 min. The metal content for 'SHR-2' ink is 68.5 % and recommended processing temperature is 120 °C/15 min as per the ink supplier. However, the tag printed using 'SHR-2' ink, sintered at 80 °C has higher RCS amplitude and lower bandwidth compared to tag printed using 'SHR-1' ink, sintered at 100 °C. The third conductive ink, 'SHR-5' ink sintered at its recommended conditions (150 °C/10 min) is able to lessen the bandwidth up to 170 MHz and increase the RCS amplitude to 12 dB. The higher metal content gives better conductivity and hence better RF performance. The details of the experimented inks are shown in Table 1. The amount of metal content claimed by the supplier of 'SHR-1' ink may not be accurate as 'SHR-2' ink is able to give better performance. The simulated bandwidth of the exper-

imented chipless RFID tag having bulk copper as its metallization for its peak at 3.9 GHz is 70 MHz. Hence, among the experimented ink, the minimum bandwidth broadening of 100 MHz is seen for 'SHR-5' ink.

A simulation was performed to evaluate the relationship between the conductivity and bandwidth of the experimented chipless RFID resonators. The simulated bandwidth of the chipless RFID resonators obtained for various conductivities is shown in Figure 9. The bandwidth of the resonator is inversely proportional to the conductivity of the printed track. For higher conductivity, the bandwidth is low.

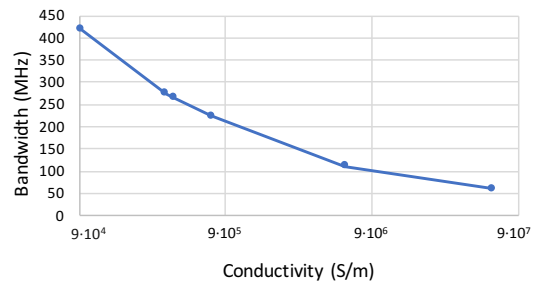


Figure 9: Simulated conductivity versus bandwidth

This means that the higher sintering temperature resulted in higher conductivity of ink and consequently, the printed tag is able to have less bandwidth broadening and better signal strength. The ink formulation in terms of metal content played a significant role in increasing the ink conductivity.

4. Photon sintering of printed RFID tags

The high volume manufacture of printed chipless RFID tags by any roll-to-roll printing process should satisfy specific industry standards. The production of the low-cost printed tag includes conductive ink printing and

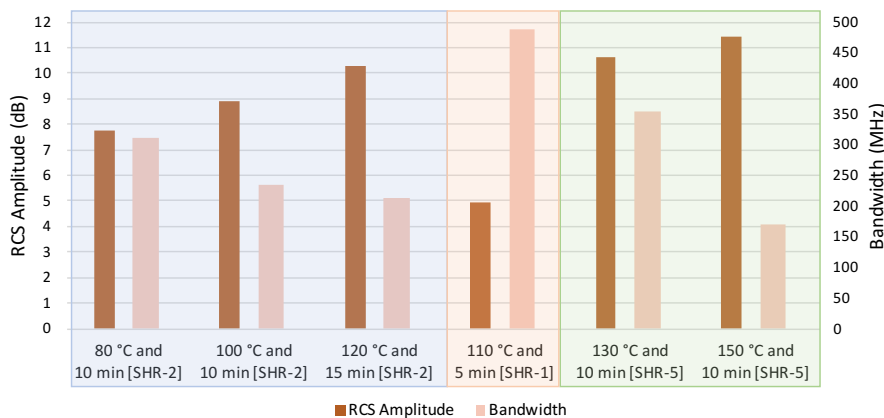


Figure 8: Microwave performance of circular ELC tag printed using 'SHR-2', 'SHR-1', and 'SHR-5' ink for different sintering temperatures

sintering process. The tags printed in the previous section were sintered using oven sintering process which requires few minutes to generate sufficient conductivity to obtain a workable printed tag. However, during the industrial manufacturing process, the sintering needs to be completed in a few seconds so that it can be suited for the roll-to-roll process. Also, most of the commercial substrates may not be able to withstand the higher temperature sintering requirement. So, a sintering process which can sinter at high temperature without altering the substrate physical properties is essential. Hence, a photonic sintering process which requires only a fraction of seconds for sintering is elucidated in this section. Optimum photon sintering conditions to obtain maximum ink conductivity is deduced after the analysis of the relation between the ink processing parameters and the electrical properties of the sintered samples.

Photonic sintering is the sintering of the printed track using high energy short pulse of light from a flash lamp. Using this technology, it is possible to attain a significantly higher temperature than the substrate can withstand in oven sintering process. In Schroder (2011), it is claimed that PET which normally has a maximum working temperature of 150 °C, can be processed at 1000 °C using photonic curing system. The pulse of light is so fast that the back side of the substrate is not heated significantly during the pulse.

The printed samples were photon-sintered using Xenon S-2100a (XENON Corporation, 2010). The S-2100a has selectable pulse duration from 100 μ s to 2000 μ s and adjustable pulse energy from 100 J to 2000 J. The lamp voltage can range from 1.6 kV to 3.0 kV with digital control. The initial photon sintering is performed on rectangular printed bars. The printed bars when sintered with the same pulse width, at the same distance gave low resistance for high voltage as seen in Table 2.

Table 2: Sheet resistivity of printed bars, photon-sintered at different voltages

Voltage (kV)	Distance (inch)	Pulse width (μ s)	Sheet resistivity (Ω /sq)
3	0.125	2000	1.913
2	0.125	2000	3.633

Then, the photon sintering is performed by placing the printed tracks at varying distance from the lamp. The distance of the sample has a significant effect on the amount of light absorbed by the sample. For instance, there will be a 60 % decrease in the energy when the sample is positioned 3 inches away from the lamp rather than 1 inch. The obtained sheet resistivity of printed bars with 400 μ m width for varying distance of the sample from the lamp is shown in Figure 10. The

distance has a linear relationship with the sheet resistance as decreasing the distance between the lamp and the sample increases the energy with which the sample is sintered as shown in Figure 10. The 9.75 inch is the shortest distance between the flash lamp and the sample and hence has the lowest sheet resistance.

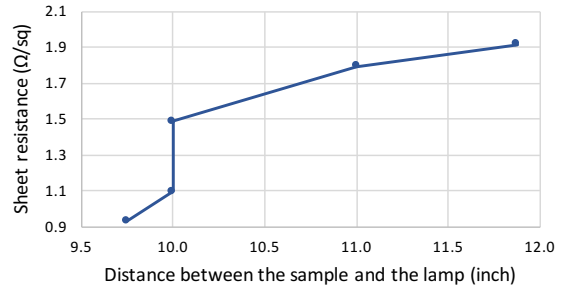


Figure 10: Sheet resistivity of printed tracks of 400 μ m width photon-sintered at varying distance from the flash lamp


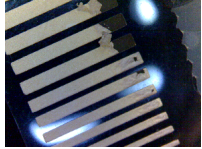
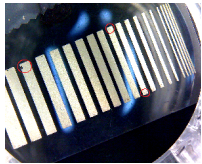
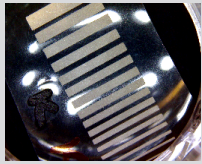

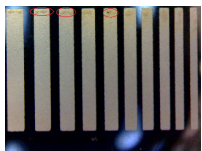
4.1 Photon sintering of chipless RFID tags printed on PET substrate

The resistance is low for higher voltage and samples near to the flash lamp, as discussed in the previous section. However, it is not practically feasible to place the sample so close to the flash lamp (9.75 inches). If ink sputtering occurs during the sintering process, then it can damage the lamps. In this section, the photon sintering of rectangular bars and chipless RFID tags is performed using covering material to avoid the sputtering of ink. The voltage is kept constant at the highest voltage (3 kV) and longest pulse width (2000 μ s) is used in sintering of all samples. The distance between the sample and the lamp is varied to find the best height of the sample so that the sample can receive uniform sintering without getting burnt.

Table 3 shows the summary of the photon sintering performed on PET substrate printed using ‘SHR-2’ ink. The Images 1 to 6 in Table 3 for sintered samples were captured using a digital microscope Dynolite (2.0 MP) with the 10 \times magnification. In this section, the single-sided and two-sided photon sintering is performed. The use of quartz covering burnt the sample (it changed into grey colour and ink bubbles were seen initially but later ink came off). The two-sided sintering with samples covered by quartz, which involves sintering from both ink side and the substrate side, is also not able to protect the sample from getting damaged. Hence, the use of quartz covering generated excessive heat during the photon sintering of the silver printed track.

When the covering lid was changed to Pyrex for the same setting, the sample was not sintered properly but bubbles were seen at the edge of the bar as seen

Table 3: Photon-sintering of printed samples using 'SHR-2' ink with voltage of 3 kV

Distance (inch)	Sintered side (Covering)	Sheet resistance (Ω/sq)	Comment	Images from Dynolite
10.0	Ink side (Quartz)	–	Sample get burnt	 Image 1: Rectangular bar 'a'
10.5	Substrate side – 1 st Ink side – 2 nd (Quartz)	–	Non-uniform sintering and sample was damaged	 Image 2: Rectangular bar 'g'
10.0	Ink side (Pyrex)	0.287	Sheet resistance is less but visually the ununiform sintering was seen	 Image 3: Rectangular bar 'b'
11.0	Ink side (Pyrex)	0.438	RF signals present for a tag with a bandwidth of 380 MHz	–
10.5	Ink side (Pyrex)	0.349	RF signals present for a tag with a bandwidth of 285 MHz	 Image 4: Rectangular bar 'k'
10.5	Ink side – 1 st Substrate side – 2 nd (Pyrex)	0.315	Visually the non-uniform sintering was seen	 Image 5: Rectangular bar 'i'
10.5	Substrate side – 1 st Ink side – 2 nd (Pyrex)	0.326	Visually the non-uniform sintering was seen	 Image 6: Rectangular bar 'h'

for rectangular bar (Image 3, in Table 3). The distance of 11 inches and 10.5 inches from the lamp gave uniform sintering. The sintering at two sides (ink side and film side) using Pyrex resulted in bubbles (Images 5 and 6, in Table 3) even though sheet resistance was less compared to other photon-sintered sample. Thus, the experimental investigation shows that the voltage of 3 kV, a distance of 10.5 inches, the pulse width of 2000 μs , Pyrex covering and one-sided photon sintering are the optimum conditions for the printed chipless tag on PET substrate

as they gave uniform sintering and low resistance compared to other samples. The microwave performance was measured for the tags that are coloured grey in Table 3. Let us consider the sample placed at 11.0 inches and 10.5 inches as 'A' and 'B', respectively. Table 4 shows the measured bandwidth and RCS difference for the measured photon-sintered tags with their corresponding sample names. Hence a detectable electromagnetic response is obtained for printed RFID tags sintered using the photon sintering process on PET substrate.

Table 4: Radar cross section and bandwidth of photon-sintered tags

Sample name	Thickness (µm)	Sheet resistance (Ω/sq)	Conductivity (S/m)	Bandwidth (MHz)	RCS (dB)
'B'	6.626	0.349	$4.32 \cdot 10^5$	285	9.51
'A'	5.696	0.438	$4.01 \cdot 10^5$	380	6.79

4.2 Comparison of photon-sintered and oven-sintered samples

The RFID tags sintered using oven and photon sintering can have variation in their conductivity and microwave performance. The sheet resistance, conductivity and mean roughness of samples printed using 'SHR-2' ink on PET substrate and sintered using the oven and photon sintering process is shown in Table 5. The photon sintering is performed with the optimum settings as explained in Section 4.1. The sintering process evaporates the dispersion solvent and sinters the left metallic particles to form conductive lines. The oven sintering process since it takes longer time is able to produce low resistance conductive line compared to photon sintering process. However, the sheet resistance is only increased by 0.3 Ω/sq when the samples are sintered

using photon sintering. The conductivity is correspondingly higher for oven sintering. The mean roughness of the printed tracks is measured using Bruker contour GT-K optical profiler. The mean roughness of rectangular bars and RFID tags is also compared in Table 5 for both sintering processes and it is seen that the roughness of the printed samples is not significantly affected by the change in sintering procedure. The microwave performance in terms of 3 dB bandwidth and RCS amplitude for tags sintered using box-oven and photon sintering is shown in Figure 11. The photon sintering of the tag performed with the samples placed at a 10.5 inch distance from the flash lamp is comparable to the oven-sintered tag at 80 °C for 10 minutes as this photon-sintered tag has rather low bandwidth and high RCS strength. The oven-sintered tag at 120 °C for 10 minutes has the best microwave response but these

Table 5: Sheet resistance, conductivity and mean roughness of oven-sintered and photon-sintered samples

Sintering process	Sheet resistance (Ω/sq)	Thickness (µm)	Conductivity (S/m)	Mean roughness (µm)
Photon sintering	0.3490	6.402	$4.48 \cdot 10^5$	1.310
	0.4380	4.300	$5.31 \cdot 10^5$	1.115
	0.4040	5.492	$4.51 \cdot 10^5$	1.184
Oven sintering (120 °C/10 min)	0.1662	5.494	$1.10 \cdot 10^5$	1.228
	0.1880	4.906	$1.08 \cdot 10^5$	1.485
	0.1810	5.330	$1.04 \cdot 10^5$	1.360

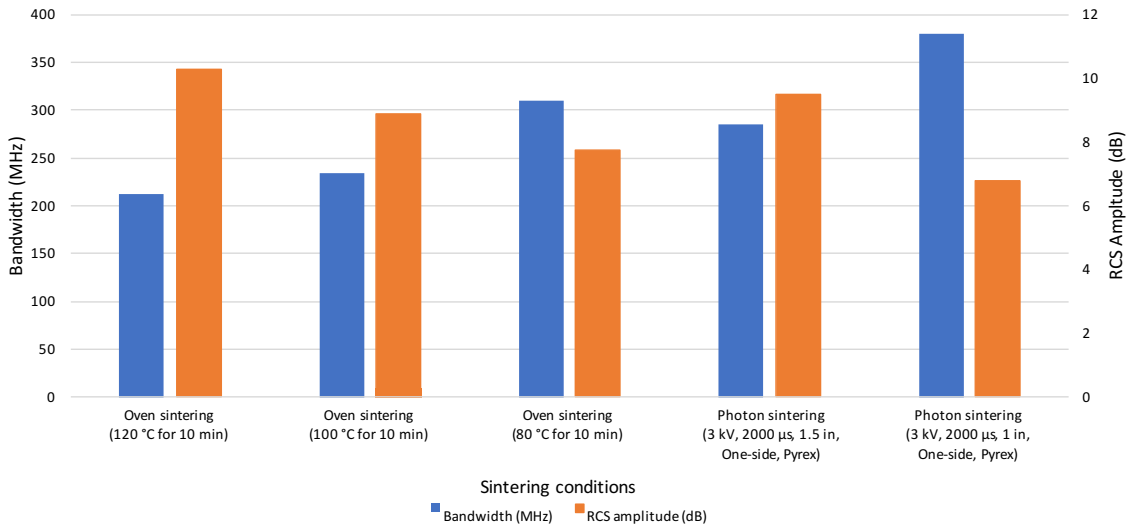


Figure 11: Microwave performance of oven-sintered and photon-sintered RFID tags (4 bit circular ELC tag printed using 'SHR-2' ink on PET substrate)

sintering conditions can be unsuitable for some commercial low-temperature substrates. The photon-sintered sample is able to obtain the lowest bandwidth of 285 MHz and the highest RCS amplitude of 9.51 which can be considered as a detectable tag ID.

4.3 Two-sided photon sintering of chipless RFID tag

In the previous section, the photon sintering is performed on a PET substrate for chipless RFID tags. The optimum settings were able to give the sheet resistance of 0.349 Ω /sq and a minimum bandwidth of 285 MHz with RCS amplitude of 9.51 dB. In this section, the photon sintering process is further optimized to obtain better RF performance and have the response comparable to the best result obtained from the oven sintering process. The photon sintering is performed on the more challenging substrate, biaxially oriented polypropylene (BOPP) polymerised with dicumyl peroxide (DCP), which cannot withstand the temperature higher than 80 °C. The issues seen in the previous section are samples getting burnt, with bubbles seen, which indicates the use of high power. Hence, to reduce the power exposed to the samples and to obtain uniform sintering, two-sided and two-times sintering has been utilized in this section. The two-sided sintering in

the previous section could not give a useful response because of high power, so in this section low voltage is tried to avoid non-uniform sintering.

In this section, the photon sintering is performed for inks with different viscosity to verify the versatility of photon sintering process. The photon sintering is performed on printed samples using three conductive inks: 'SHR-1', 'SHR-2', and 'SHR-4'. The viscosity of these inks and their wet ink layer thickness measured using Bruker contour GT-K optical profiler is shown in Table 6. The viscous ink deposits lower thickness compared to less viscous ink. The highest thickness was achieved with the ink 'SHR-4'.

Table 6: Thickness of printed samples for different inks

Ink name	Viscosity (Pa-s)	Sample description	Wet thickness (μ m)
SHR-1	29.0	Not pre-dried sample	3.894
		Pre-dried sample	5.008
SHR-2	17.5	Not pre-dried sample	5.404
		Pre-dried sample	5.350
SHR-4	15.0	Not pre-dried sample	7.386
		Pre-dried sample	7.544

Table 7: Photon sintering of samples printed using 'SHR-2' ink on BOPP DCP substrate (distance = 1.5 inches from the lamp)

Sintering condition	No. of passes	Pulse width (μ s)	Voltage (kV)	Sintered side	Sheet resistance (Ω /sq)
Photon-sintered (printed samples are not pre-dried)	1	2000	3.0	Coating	Uneven sintering
	2	2000	2.0	Coating	Burnt
			3.0	Film	
	2	2000	2.5	Coating	0.277
			2.5	Film	
	2	2000	2.0	Coating	0.308
			2.5	Coating	
	2	2000	2.5	Coating	0.290
			3.0	Coating	
	2	1000	3.0	Coating	0.305
		2.0	Coating		
	2	2000	2.5	Coating	0.275
		2.5	Film		
Photon-sintered on samples pre-dried at 80 °C for 15 s	2	2000	2.0	Coating	0.392
		1000	3.0	Film	
	2	2000	2.5	Coating	0.260
			2.5	Film	
	2	2000	2.0	Coating	0.349
			2.5	Coating	
	2	2000	2.5	Coating	0.320
			3.0	Coating	
	2	2000	2.5	Coating	0.222
		2.5	Film		

Initially, the sintering trials were done with rectangular bars and a sheet resistance of rectangular bar was measured to analyze the sintering performance. The distance and cover lid material have been kept constant as 10.5 inches and Pyrex, respectively. The power was changed to three different level: 3 kV, 2.5 kV, and 2 kV. These three power levels can be considered as High, Medium and Low power levels, respectively. We cannot go lower than 2 kV power using the Xenon S-2100a photonic sintering.

The printed side can be mentioned as coating side and non-printed side as film side. The two-sided sintering and two-pass sintering are done for two different voltage conditions. The sintering is performed for wet samples and samples pre-dried using oven sintering at 80 °C for 15 s. The sheet resistance obtained for different sintering conditions is shown in Table 7, Table 8, and Table 9, respectively.

The optimum conditions for the PET sample (3 kV, 10.5 inches) brought uneven sintering for BOPP sample. Then, two-sided sintering is performed with 2 kV (Low) for coating side and 3 kV (High) for film side which also resulted in the burnt sample. The voltage is then reduced to medium (2.5 kV) and two-sided sintering is performed and a low-resistance sintered sample is obtained. The sheet resistance obtained for non-pre-

dried and predried samples printed using ‘SHR-2’ ink for varying pulse width and voltage is shown in Table 7 and it can be seen that the minimum sheet resistance is obtained for sintering of coating and film side with 2.5 kV (Medium) and 2000 μs pulse width, which is highlighted by the grey background.

The obtained sheet resistance values for both ‘SHR-1’ and ‘SHR-4’ inks are also lowest for the same conditions (two-sided sintering with the medium voltage at 2000 μs pulse width) as seen in Table 8 and Table 9, also highlighted by the grey background.

The interpretation of microwave performance in terms of RCS amplitude and bandwidth of RFID tag sintered using photon sintering and oven sintering is shown in Table 10. The photon sintering of samples printed using ‘SHR-2’ ink reduced the bandwidth to 220 MHz with RCS amplitude of 12.42 dB, which is comparable to the response obtained from oven sintering. The sheet resistance has decreased by 0.1 Ω/sq compared to one-sided sintering performed in the previous section. In case of ‘SHR-1’ ink, the response of the printed tag is rather enhanced for the photon-sintered sample as oven sintering is limited to 80 °C for BOPP substrate. This can be related to the sheet resistance decrement by 0.5 Ω/sq for the photon-sintered sample. The samples printed using ‘SHR-4’ ink have higher thickness compared to

Table 8: Photon sintering of samples printed using ‘SHR-1’ ink on BOPP DCP substrate with two passes (distance = 1.5 inches from the lamp)

Sintering condition	Pulse width (μs)	Voltage (kV)	Sintered side	Sheet resistance (Ω/sq)
Photon-sintered only (printed samples are not pre-dried)	2000	2.0	Coating	0.752
	1000	3.0	Film	
	2000	2.5	Coating	0.476
		2.5	Film	
	2000	2.0	Coating	0.734
		2.5	Coating	
	2000	2.5	Coating	0.605
		3.0	Coating	
	2000	2.5	Coating	0.526
		2.5	Film	
Photon-sintered on samples pre-dried at 80 °C for 15 s	2000	2.0	Coating	0.759
	1000	3.0	Film	
	2000	2.5	Coating	0.526
		2.5	Film	
	2000	2.0	Coating	0.711
		2.5	Coating	
	2000	2.5	Coating	0.608
		3.0	Coating	
	2000	2.5	Coating	0.506
		2.5	Film	

Table 9: Photon sintering of samples printed using ‘SHR-4’ ink on BOPP DCP substrate with two passes (distance = 1.5 inches from the lamp)

Sintering condition	Pulse width (μs)	Voltage (kV)	Sintered side	Sheet resistance (Ω/sq)
Photon-sintered only (printed samples are not pre-dried)	2000	2.0	Coating	Uneven sint.
	2000	3.0	Film	
	2000	2.5	Coating	0.277
		2.5	Film	
	2000	2.0	Coating	0.349
		2.5	Coating	
	2000	2.0	Coating	0.398
		3.0	Coating	
	1000	3.0	Coating	
	2000	2.5	Coating	0.313
	2.5	Film		
Photon-sintered on samples pre-dried at 80 °C for 15 s	2000	2.0	Coating	0.392
	1000	3.0	Film	
	2000	2.5	Coating	0.265
		2.5	Film	
	2000	2.0	Coating	0.389
		2.5	Coating	
	2000	2.5	Coating	0.359
		3.0	Coating	
	2000	2.5	Coating	0.252
		2.5	Film	

Table 10: Microwave performance of circular ELC resonator sintered using photon-sintering and oven-sintering procedures

Ink	Sintering method	Sheet resistance (Ω/sq)	Bandwidth (MHz)	RCS amplitude (dB)
SHR-2	Photon-sintered only (not pre-dried)	0.275	230	12.42
	Photon-sintered (pre-dried 80 °C for 15 s)	0.222	220	12.42
	Oven-sintered (80 °C for 10 min)	0.385	230	12.47
SHR-1	Photon-sintered only (not pre-dried)	0.526	290	8.16
	Photon-sintered (pre-dried 80 °C for 15 s)	0.506	270	9.38
	Oven-sintered (80 °C for 10 min)	1.076	350	7.17
SHR-4	Photon-sintered only (not pre-dried)	0.313	320	8.41
	Photon-sintered (pre-dried 80 °C for 15 s)	0.252	360	6.75
	Oven-sintered (80 °C for 10 min)	0.288	220	13.95

other inks as shown in Table 6, which can be the reason to have better performance for oven-sintered sample compared to photon-sintered sample. The higher thickness of ‘SHR-4’ ink might have been sintered more uniformly using oven sintering than photon sintering.

Hence, the photon sintering has shown improvement for RFID tag printed using ‘SHR-1’ ink. The microwave performance for sample printed using ‘SHR-2’ ink is similar for oven-sintered and photon-sintered sample. However, oven-sintered printed sample using ‘SHR-4’ ink is better compared to photon-sintered sample because of higher layer thickness. A high-speed photonic curing system is applicable for chipless RFID printed system and can be readily used to manufacture workable tag using fast roll-to-roll printing process.

5. Effect of the printed tracks dimensions on electrical parameters

The resistance of printed track depends on ink material composition, printing technology and geometrical dimensions (Bonea, et al., 2012). The wider line is less resistive and has higher conductivity based on the experimental investigation shown in Figure 12.

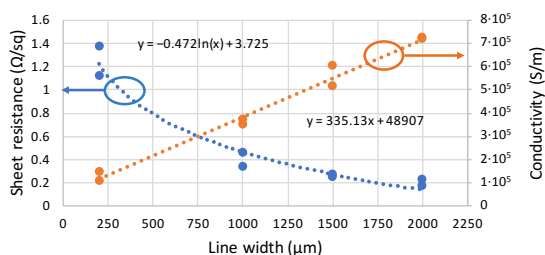


Figure 12: Sheet resistance and conductivity for varying line width of the track printed using ‘SHR-2’ ink

This is because the homogeneity of the conductive layer is better for the wider strip. It is seen that the conduc-

tivity gets decreased by $5 \cdot 10^5$ S/m when the line width is decreased from 2000 μm to 200 μm. However, the conductivity in the range of 10^5 is still maintained for the narrowest strip of 200 μm line width. The resistance should be low enough even for narrower strips to obtain detectable microwave response. The fitted relationship between sheet resistance and conductivity, respectively, and the line width is shown in Equations [2] and [3], which can be used to predict the printed line conductivity for different line widths (in μm).

$$\text{Sheet resistance} = -0.472 \ln(\text{linewidth}) + 3.725 \quad [2]$$

$$\text{Conductivity} = 335.13 \times \text{linewidth} + 48907 \quad [3]$$

The experimental investigation performed in previous paragraph showed that the conductivity of printed strip is dependent on the ink width and the deposited ink thickness. The geometrical dimensions, i.e. the line length, width and ink thickness give the total amount of ink volume of a printed strip. This section investigates the effect of overall ink volume on the conductivity of the printed strip. The sheet resistance and conductivity of strip printed using ‘SHR-2’ ink of varying ink volume are depicted in Figure 13.

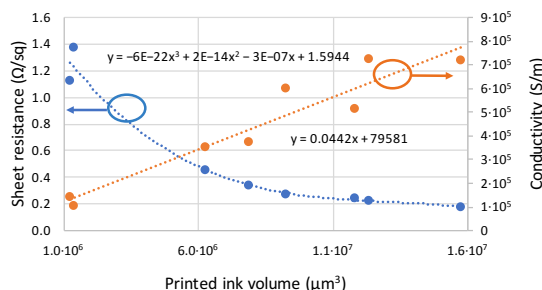


Figure 13: Sheet resistance and conductivity of strip printed using ‘SHR-2’ ink of varying ink volume

The conductivity is directly proportional to the printed ink volume, which indicates that the bigger tag design

with higher ink deposition has better conductivity compared to compact tag design. The chipless tag design is moving towards the development of smaller tags in order to have higher spatial efficiency. In case of the printed version of the chipless tag, the smaller tags can suffer because of low conductivity based on the relationship shown in Figure 13.

6. Printed samples accuracy

This section investigates the line width and gap width uniformity for printed samples on BOPP and PET substrate. The printed line width and the gap width of the chipless tag are measured using a Leica DM2500 microscope. The actual line width and gap width of the tag are 300 μm and 200 μm, respectively. The line width and the gap width of the resonator can vary after printing because of ink spreading or low ink flow. The width discrepancy for measured line width of 300 μm and gap discrepancy for measured gap width of 200 μm, are calculated using measured printed widths. The measurement is done for chipless tags printed on PET and BOPP substrate and the obtained discrepancy is shown in Figure 14.

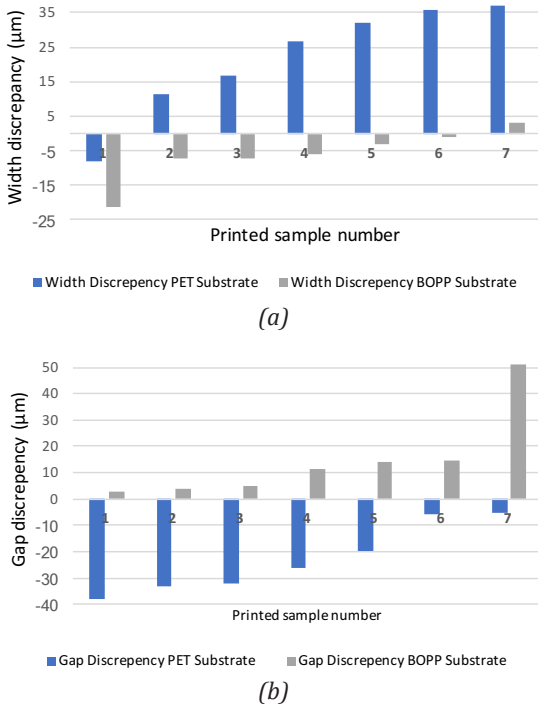


Figure 14: Line width (a) and gap width (b) discrepancy for RFID tags printed on PET and BOPP

In case of PET, the most part of the resonator has width widening causing a smaller gap (hence negative for gap discrepancy value) with the maximum of width increment of 37 μm. In the case of BOPP, the printed

lines have lower width than is the designed width of the sample, increasing the gap compared to the desired one. The deviation of the width increasing or gap narrowing in PET is lower compared to BOPP which can be because of the higher adhesion to PET. The reason behind the inconsistent discrepancy in line width and gap width can be because of variation in printing pressure, ink amount, and substrate flatness during manual screen printing. The automatic screen printing is able to minimize this discrepancy to a certain extent.

The resonant frequency of the tag is dependent on the equivalent inductance and the capacitance of the printed strip and the change in line width or the gap width of the printed strip can bring the change in resonant frequency. For instance, in BOPP printed sample number 1, the width is varied by 20 μm as seen in Figure 14(a). So, the simulation of the 1-bit RFID tag for the width of 280 μm and 300 μm is performed in Figure 15. The frequency shift is seen and hence printing accuracy is essential for detecting correct tag identification in printed RFID tag.

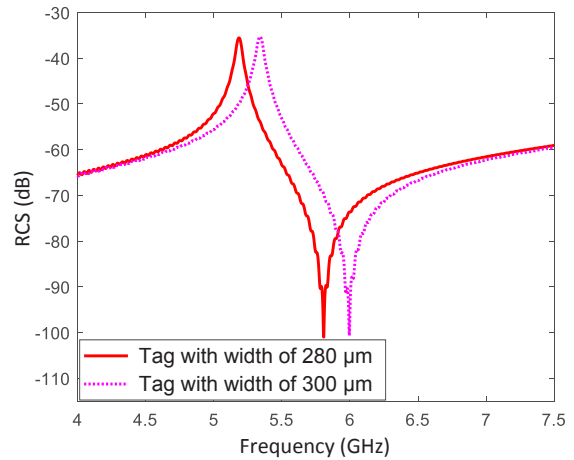


Figure 15: Response of the chipless RFID tag with different widths

We can assume the average line width broadening as *IncWidth* and decreased gap width as *DecGap* and consider these values in next print with smaller line width and reprint them to have the desired width. Hence, the adjusted line width and gap width can be obtained from Equations [4] and [5], respectively. For instance, for circular tag printed on PET, the average width broadening *IncWidth* is 21.65 μm and average gap decrease *DecGap* is 22.87 μm. These values can be considered in a new print to obtain required resonator dimensions.

$$\text{New line width} = \text{Old line width} - \text{IncWidth} \quad [4]$$

$$\text{New gap width} = \text{Old gap width} + \text{DecGap} \quad [5]$$

7. Relationship between printed tag response and printing parameters

This section will summarise the understanding obtained from the experimental analysis performed in the previous section and propose a general guidelines for printing of chipless tags. The microwave performance of printed chipless RFID tag is dependent on various printing parameters. A dependency chart showing the inter-relationship between the various printing parameters and the microwave performance of the printed tag is shown in Figure 16.

The microwave performance of printed tag is mainly dependent on four parameters: deposited ink thickness, ink conductivity, printing accuracy, and substrate parameters. The deposited ink thickness is dependent on the printing method and ink viscosity. The ink with higher viscosity can deposit higher ink thickness. However, the printing technique also determines the viscosity of the ink. The higher ink thickness is required for better RF response as explained in Section 2.

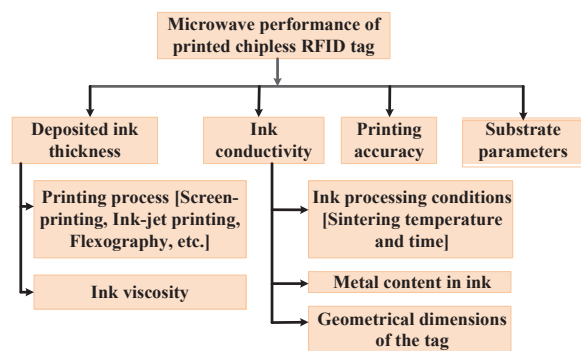


Figure 16: Relationship between the parameters involved in the printing of chipless RFID tag with its microwave performance

The screen-printing process can deposit a higher amount of ink compared to other printing processes. However, multiple passes can be printed in other print-

ing processes to increase the deposited ink thickness. The printing process needs to be automatic to implement the multiple-pass print. Also, the excess amount of ink can create ink smudging and ink overflow creating unnecessary shorting. So, the ink viscosity needs to be optimal to print strip with higher thickness and better accuracy.

The low conductivity of ink broadens the microwave signal of the printed tag and also decreases the signal strength. Based on the experimental analysis higher sintering temperature can remove a greater amount of resistive component from the ink, forming highly conductive printed lines. However, the sintering temperature is limited by the physical properties of the substrate. The amount of metal content also has an influence on the ink conductivity.

Therefore, the bandwidth broadening for printed RFID tag can be minimized by using conductive ink which can give high conductivity at low sintering temperature for the oven sintering process. This will allow having printed RFID tag on a substrate with a low melting point. The photon sintering process can be adapted to have fast sintering for these substrates.

The geometrical dimensions (printed area) have a significant effect on the conductivity of the printed line according to the experimental investigation. The compact size tag is required to have higher bit capacity in the smaller area, which needs high resolution of printing. The digital printing technique such as ink-jet printing is able to print fine lines compared to the screen-printing technique. The multiple passes of print need to be employed to have higher ink thickness deposition which will reduce the resistance and minimize the signal loss as explained in Section 2. The printing accuracy is also important to obtain desired microwave response. The resonators are usually detuned using shorting at different locations. The printing inaccuracy due to ink overflow can create unwanted shorting in these locations and detune the resonator resulting in

Table 11: Issues, reasons, and solutions of the printed tags

Issue	Reason	Solution
Bandwidth broadening (low spectral efficiency)	Low ink conductivity	Ink sintered at a higher temperature for oven sintering or two-sided photon sintering
Low signal strength (RCS amplitude)	Low metal content	Select ink with solid content >50 %
	Low ink layer thickness	Screen print can deposit higher thickness or use multiple passes for other printing technologies
The need of larger print dimensions Printed dimensions inaccuracy	Low ink viscosity	Increase the ink viscosity
	Low ink conductivity	Use ink with high conductivity
	Printing technology	Use of digital printing technology; print the resonator with adjusted dimensions (considering the offset due to printing)

the false negative of the tag ID. The uniformity of line width in all sections of the printed resonator can also get affected because of printing inaccuracy which can result in false tag ID or absence of tag ID.

The screen-printing technique is prone to printing inaccuracy compared to other printing techniques. The printing accuracy can be enhanced by determining the change in printed dimensions and incorporating it in next print. The digital printing process such as ink-jet printing technique can be adapted to have better accuracy in printed dimensions. The summary of the analyzed issues of the printed RFID tag with their reason and the solution is shown in Table 11.

8. Conclusion

The printable chipless RFID tag combining the use of high-throughput printing processes and low-cost substrates such as a polymer is the most viable option to obtain extremely inexpensive RFID tags (0.1 cents/tag). The electromagnetic signature of the printed RFID tag suffers because of unavoidable limitation of printing technology. However, the performance of the printed

chipless RFID tags can be improved by understanding the bottlenecks of the manufacturing procedure of printed tags. The microwave performance of the printed tags is dependent on parameters involved in their fabrication. The relationship between the printing parameters and the microwave response was analysed comprehensively in this paper, to understand the reasons behind the issues related to printed RFID tag. The dependency of parameters involved in the printing of chipless tag with its microwave response is deduced in the final section to elaborate the relationship and propose a viable solution to enhance the detection from the printed tag. An optimum printing setup, giving the workable tag response, can be deduced with the aid of this relationship which will eventually assist in obtaining a detectable and consistent response from the printed tag. The photon sintering of the chipless RFID tag is performed for the first time, to verify its suitability and obtain optimum conditions which can give the best microwave response. The photon sintering process can support sintering in a few seconds, making it suitable for the commercial roll-to-roll process of manufacturing printed items. This process can sinter the printed tracks at a temperature higher than the melting point of the substrate.

Acknowledgement

We acknowledge Dr. Phei Lok from CCL secure for her constant guidance and support. We are grateful to CCL Secure, Australia for providing the screen-printing and equipment facilities. We wish to thank Dr. Anthony Chesman from CSIRO for his help in photon sintering of printed samples.

References

- Balbin, I. and Karmakar, N.C., 2009. Phase-encoded chipless RFID transponder for large-scale low-cost applications. *Microwave and Wireless Components Letters, IEEE*, 19(8), pp. 509–511.
- Bonea, A., Brodeala, A., Vlădescu, M. and Svasta, P., 2012. Electrical conductivity of inkjet printed silver tracks. In: *2012 35th International Spring Seminar on Electronics Technology (ISSE 2012)*. Bad Aussee, Austria, 9–13 May 2012. IEEE, pp. 1–4.
- Borgese, M., Dicandia, F.A., Costa, F., Genovesi, S. and Manara, G., 2017. An inkjet printed chipless RFID sensor for wireless humidity monitoring. *IEEE Sensors Journal*, 17(15), pp. 4699–4707.
- Chamarti, A. and Varahramyan, K., 2006. Transmission delay line based ID generation circuit for RFID applications. *IEEE Microwave and Wireless Components Letters*, 16(11), pp. 588–590.
- Das, R. and Harrop, P., 2010. Printed and chipless RFID forecasts, technologies & players. [online] Available at: <https://www.idtechex.com/research/reports/printed_and_chipless_rfid_forecasts_technologies_and_players_2009_2019_000225.asp> [Accessed September 2018].
- Forouzandeh, M. and Karmakar, N.C., 2015. Chipless RFID tags and sensors: a review on time-domain techniques. *Wireless Power Transfer*, 2(2), pp. 62–77.
- Genovesi, S., Costa, F., Monorchio, A. and Manara, G., 2014. Phase-only encoding for novel chipless RFID tag. In: *2014 IEEE RFID Technology and Applications Conference (RFID-TA)*. Tampere, Finland, 8–9 September 2014. IEEE, pp. 68–71.
- Genovesi, S., Costa, F., Monorchio, A. and Manara, G., 2016. Chipless RFID tag exploiting multifrequency delta-phase quantization encoding. *Antennas and Wireless Propagation Letters*, 15, pp. 738–741.
- Halonen, E., Viiru, T., Ostman, K., Cabezas, A.L. and Mäntysalo, M., 2013. Oven sintering process optimization for inkjet-printed Ag nanoparticle ink. *IEEE Transactions on Components, Packaging and Manufacturing Technology*, 3(2), pp. 350–356.
- Herrojo, C., Mata-Contreras, J., Paredes, F., Núñez, A., Ramon, E. and Martín, F., 2018. Near-field chipless-RFID tags with sequential bit reading implemented in plastic substrates. *Journal of Magnetism and Magnetic Materials*, 459, pp. 322–327.

- Huang, H.-F. and Su, L., 2017. A Compact Dual-Polarized Chipless RFID Tag by Using Nested Concentric Square Loops. *IEEE Antennas and Wireless Propagation Letters*, 16, pp. 1036–1039.
- Jeon, D., Kim, M.-S., Ryu, S.-J., Lee, D.-H. and Kim, J.-K., 2017. Fully printed chipless RFID tags using dipole array structures with enhanced reading ranges. *Journal of Electromagnetic Engineering And Science*, 17(3), pp. 159–164.
- Khan, M.M., Tahir, F.A. and Cheema, H.M., 2016. Frequency band utilization enhancement for chipless RFID tag through place value encoding. In: *2016 IEEE International Symposium on Antennas and Propagation (APSURSI)*. Fajardo, Puerto Rico, 26 June–1 July 2016. IEEE, pp. 1477–1478.
- Lukacs, P., Pietriková, A. and Cabuk, P., 2017. Dependence of electrical resistivity on sintering conditions of silver layers printed by inkjet printing technology. *Circuit World*, 43(2), pp. 80–87.
- Mandel, C., Schüßler, M., Nickel, M., Kubina, B., Jakoby, R., Pöpperl, M. and Vossiek, M., 2015. Higher order pulse modulators for time domain chipless RFID tags with increased information density. In: *2015 45th European Microwave Conference (EuMC)*. Paris, 7–10 September 2015. EuMA, pp. 100–103.
- Naqui, J., Coromina, J., Martín, F., Horestani, A. K. and Fumeaux, C., 2014. Comparative analysis of split ring resonators (SRR), electric-LC (ELC) resonators, and S-shaped split ring resonators (S-SRR): potential application to rotation sensors. In: M. Essaaidi, ed. *Proceedings of 2014 Mediterranean Microwave Symposium (MMS2014)*. Marrakech, Morocco, 12–14 December 2014. IEEE.
- Noor, T., Habib, A., Amin, Y., Loo, J. and Tenhunen, H., 2016. High-density chipless RFID tag for temperature sensing. *Electronics Letters*, 52(8), pp. 620–622.
- Preradovic, S. and Karmakar, N.C., 2009. Design of fully printable planar chipless RFID transponder with 35-bit data capacity. In: *European Microwave Week 2009, EuMW 2009: Science, Progress and Quality at Radiofrequencies, Conference Proceedings – 39th European Microwave Conference, EuMC 2009*. Rome, Italy, 28 September – 2 October 2009, pp. 13–16.
- Sajitha, V.R., Nijas, C.M., Roshna, T.K., Vasudevan, K. and Mohanan, P., 2016. Compact cross loop resonator based chipless RFID tag with polarization insensitivity. *Microwave and Optical Technology Letters*, 58(4), pp. 944–947.
- Schroder, K.A., 2011. Mechanisms of photonic curing™: processing high temperature films on low temperature substrates. In: M. Lafon and B. Romanowicz, eds. *NSTI Nanotech 2011 proceedings: Vol. 2, Nanotechnology 2011: electronics, devices, fabrication, MEMS, fluidics and computational*. Boca Raton: CRC Press, pp. 220–223.
- Vena, A., Babar, A.A., Sydänheimo, L., Tentzeris, M.M. and Ukkonen, L., 2013. A novel near-transparent ASK-reconfigurable inkjet-printed chipless RFID tag. *IEEE Antennas and Wireless Propagation Letters*, 12, pp. 753–756.
- Vena, A., Sydänheimo, L., Ukkonen, L. and Tentzeris, M.M., 2014. A fully inkjet-printed chipless RFID gas and temperature sensor on paper. In: *2014 IEEE RFID Technology and Applications (RFID-TA) Conference*. Tampere, Finland, 8–9 September 2014. IEEE, pp. 115–120.
- XENON Corporation, 2010. *Xenon S-2100: Rack-Mounted Sintering System*. [online] Available at: <https://www.polytec.com/fileadmin/d/Klebeprodukte/S-2100_SellSheet_1.pdf> [Accessed September 2018].
- Zomorodi, M., 2015. *mm-wave EM-imaging chipless RFID system*. Ph.D. Thesis. Monash University.

